ELSEVIER

International Journal of Mass Spectrometry 220 (2002) 359–374

International Journal of Mass Spectrometry

www.elsevier.com/locate/ijms

A photoionisation mass spectrometry study of the fragmentation of silicon tetrafluoride, tetrachloride and tetrabromide

L. Cooper[a], E.E. Rennie[b], L.G. Shpinkova[c], D.M.P. Holland[d,*], D.A. Shaw[d]

[a] *Department of Chemistry, Heriot-Watt University, Riccarton, Edinburgh EH14 4AS, UK*
[b] *Department of Surface Physics, Fritz-Haber Institute, Faradayweg 4-6, D-14195 Berlin, Germany*
[c] *Department of Nuclear Spectroscopy Methods, Institute of Nuclear Physics, Moscow State University, Moscow 119899, Russia*
[d] *Daresbury Laboratory, Daresbury, Warrington, Cheshire WA4 4AD, UK*

Received 4 March 2002; accepted 8 July 2002

Abstract

A time-of-flight (TOF) mass spectrometry study has been carried out to investigate the fragmentation processes occurring in SiX_4 (X = F, Cl or Br). Synchrotron radiation has been used to record spectra in the photon energy range 10–210 eV, and appearance energies have been determined for 31 singly or doubly charged fragment ions. These have enabled upper limits for, previously unknown, heats of formation to be estimated for several doubly charged atomic and molecular fragments. The TOF spectra show that the peaks due to some of the small fragments change shape as a function of excitation energy, and that at high photon energy several of the peaks consist of two components, one of which is narrow and the other broad. The latter component is due to fragments possessing substantial initial kinetic energy. The peak shape is discussed in relation to the initial formation of a doubly or triply charged parent ion, and a subsequent Coulomb repulsion. (Int J Mass Spectrom 220 (2002) 359–374)

Keywords: Time-of-flight mass spectrometry; Heats of formation; Kinetic energy release; Doubly charged ions

1. Introduction

The electronic structure and molecular bonding properties of the highly symmetric (T_d symmetry) silicon tetrahalides have attracted considerable attention. Much of this interest arises from the distinctive molecular environment experienced by the central Si atom due to the surrounding shell of electronegative atoms. The potential barrier created by this cage of halogen atoms has been invoked to interpret the unusual features observed in the photoabsorption spectra of the silicon tetrahalides [1,2]. Most of the previous photoionisation studies on these molecules have involved SiF_4, and yield curves for the production of the parent and fragment ions have been measured following valence or inner shell excitation. Appearance energies for some of the fragments, SiF_n^+ or SiF_n^{2+}, have also been determined although these measurements are far from being complete. Our knowledge of the thermochemical properties and fragmentation mechanisms for the heavier silicon tetrahalides is less satisfactory. Little information is currently available regarding the fragment ion appearance energies for $SiCl_4$, and the corresponding data for $SiBr_4$ are limited to the singly charged species.

* Corresponding author. E-mail: d.m.p.holland@dl.ac.uk

1387-3806/02/$ – see front matter
PII S1387-3806(02)00822-9

In the present study, a TOF mass spectrometer has been used with monochromated synchrotron radiation to record ion TOF spectra in the photon energy range 10–210 eV. The spectra have enabled the appearance energy (AE) of each fragment ion, formed through photoionisation or ion-pair production, of SiX_4 to be determined. In some cases the specific fragmentation process leading to the formation of a particular ion has been inferred by comparing the AE with the corresponding thermochemical threshold. In addition, an analysis of the ion TOF peak shape has allowed the initial kinetic energy possessed by a particular fragment to be deduced.

A variety of TOF techniques has been used to investigate fragmentation processes in SiF_4, and of direct relevance to the present work are photoionisation studies using pulsed [3] and static [4,5] ion extraction fields, and dipole (e, e + ion) coincidence spectroscopy studies [6,7]. However, the emphasis of these earlier studies lay in the measurement of ion yield curves and not in the determination of fragment ion AEs. Photoion–photoion coincidence experiments have been carried out to study the dissociation of SiF_4^{2+} into two singly charged fragments [3,4], and the decay dynamics of the valence states of SiF_4^+ and $SiCl_4^+$ have been investigated in the photon energy range 11–26 eV using threshold photoelectron–photoion coincidence spectroscopy [8,9]. The parent and fragment ion yield curves of $SiBr_4^+$ have been measured using photoionisation mass spectrometry in the photon energy range 10–31 eV [10].

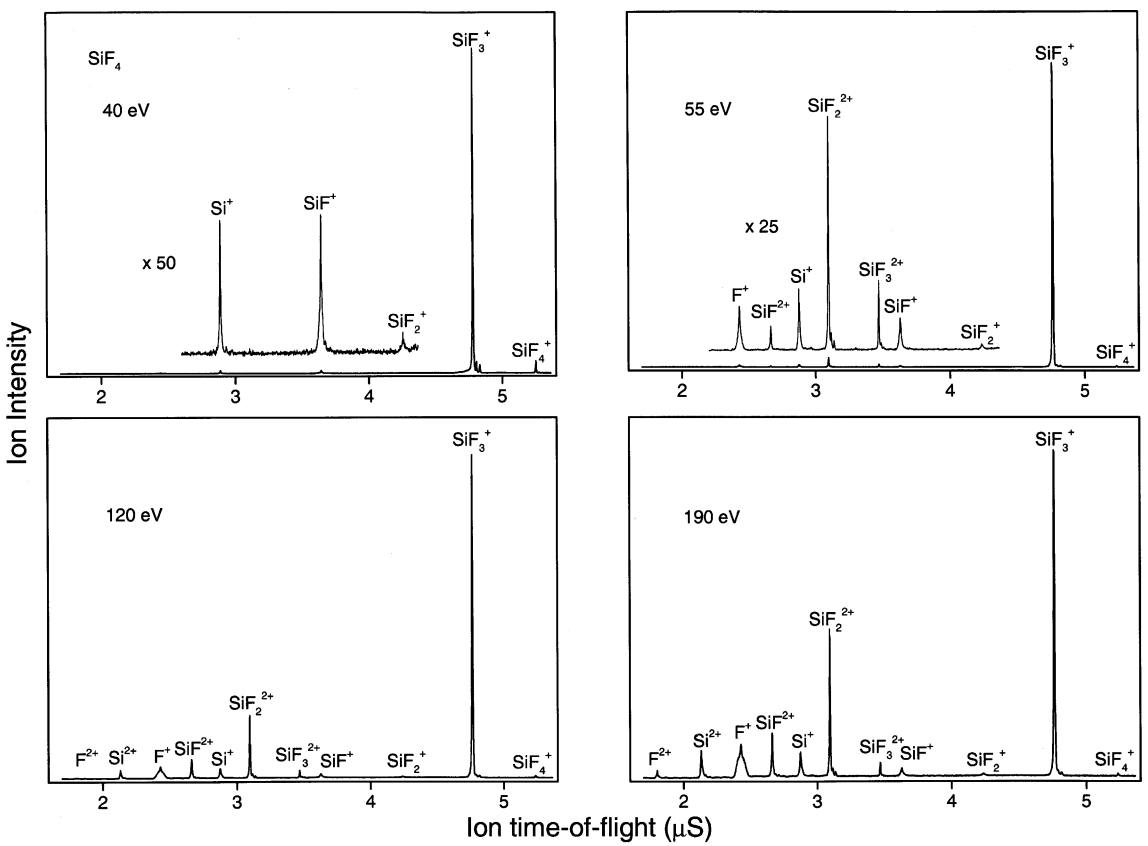

Fig. 1. Ion time-of-flight spectra of silicon tetrafluoride recorded at photon energies of 40, 55, 120 and 190 eV.

2. Experimental apparatus and procedure

The experiments were carried out at the Daresbury Laboratory synchrotron radiation source using a TOF mass spectrometer [11] attached to either a 5m normal incidence monochromator [12] or a spherical grating monochomator [13]. As the experimental apparatus and procedure have been described in detail previously, only a brief account will be given here.

Photoionisation occurs in the spectrometer source region where the monochromatic radiation intersects, perpendicularly, with a beam of the gas under investigation. A high voltage pulse, with a repetition rate of ~400 Hz, is applied across the source region to extract the ions and propel them towards the drift tube. The time between the application of this pulse and the detection of an ion was measured electronically, with the summation of many events producing a TOF spectrum. The ions were detected using a pair of channelplates, floated at ~6 kV, to minimise the variation in the detector sensitivity to ionic mass [14]. Lithium fluoride, indium, magnesium or aluminium filters, located between the monochromator exit slit and the spectrometer, could be inserted into the photon beam to partially suppress higher order radiation. Figs. 1–3 display a selection of TOF spectra for SiF_4, $SiCl_4$ and $SiBr_4$, respectively, to illustrate the variation in the fragmentation as a function of photon energy. The mass resolution is sufficient for the contributions due to the various isotopes to be observed, and, for convenience, Table 1 lists the isotopic abundances of the relevant elements. TOF spectra were recorded in the photon energy range 10–210 eV using the following energy increments: 0.05 eV (10 eV $< h\nu <$ 25 eV),

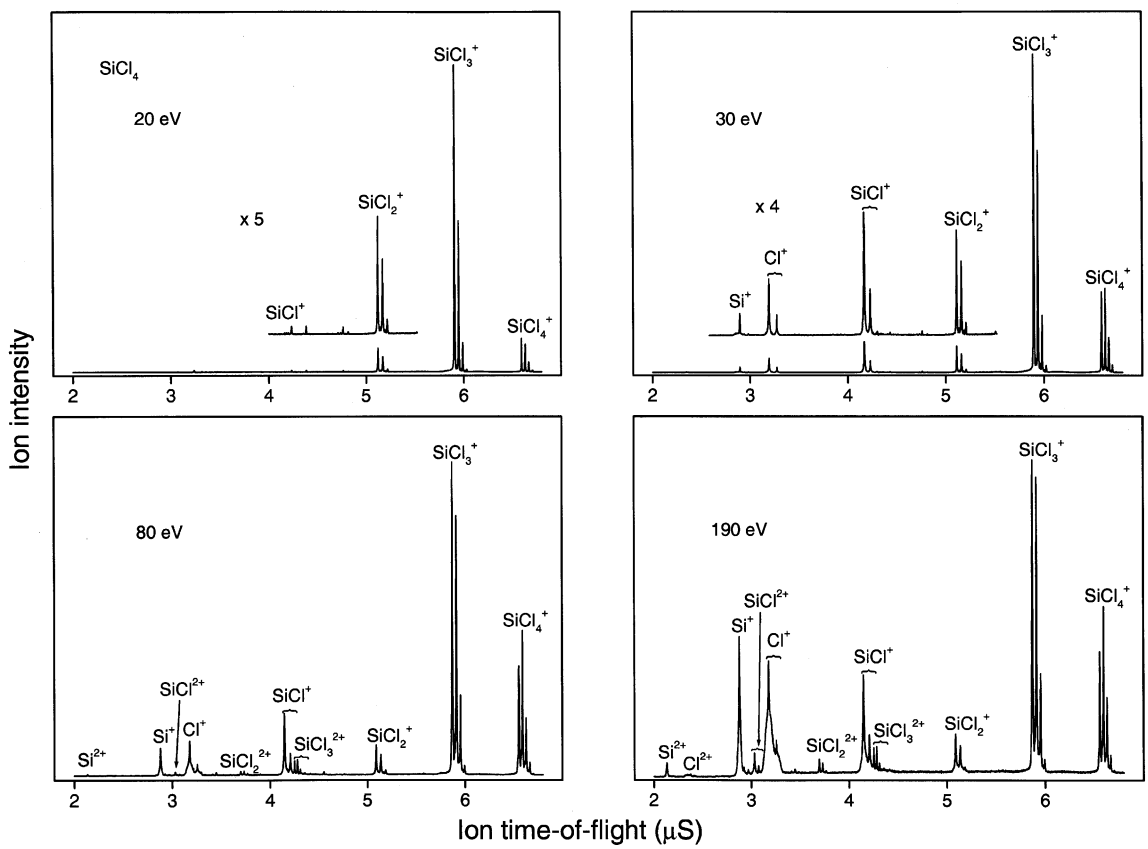

Fig. 2. Ion time-of-flight spectra of silicon tetrachloride recorded at photon energies of 20, 30, 80 and 190 eV.

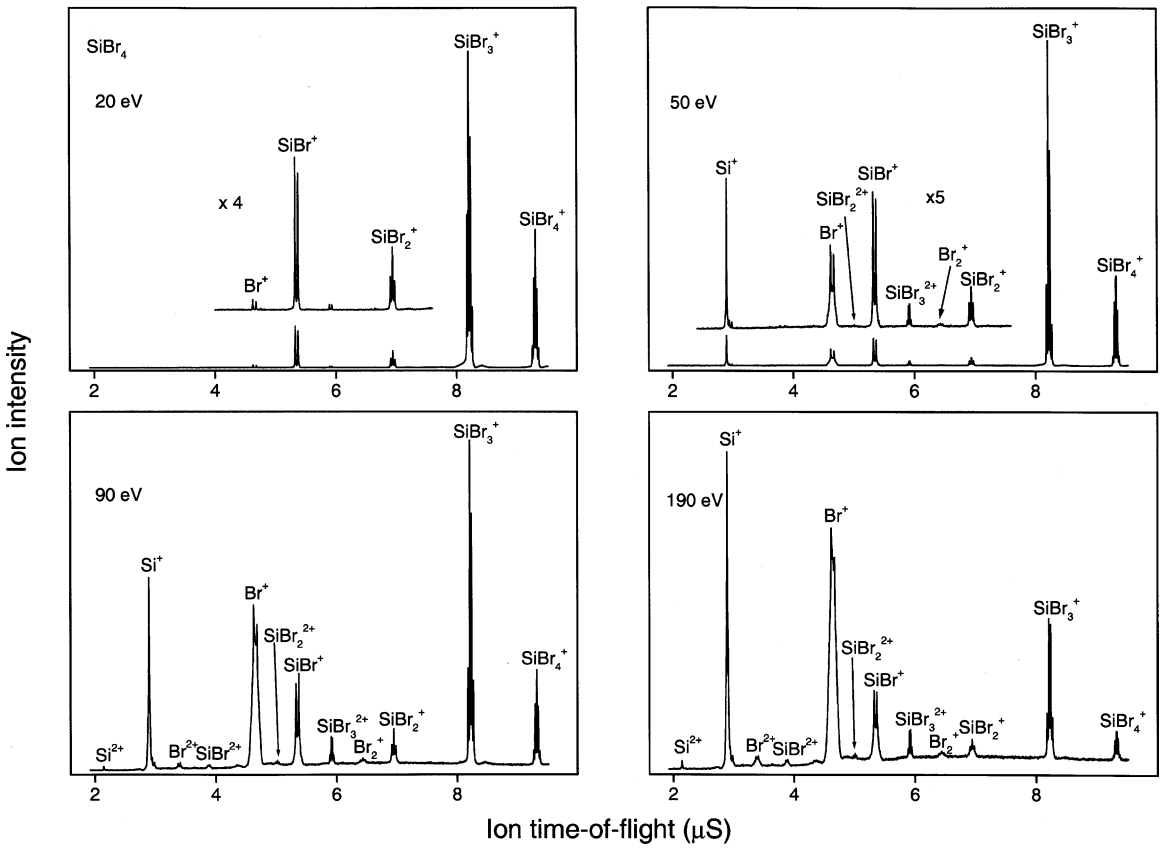

Fig. 3. Ion time-of-flight spectra of silicon tetrabromide recorded at photon energies of 20, 50, 90 and 190 eV.

0.1 eV (25 eV $< h\nu <$ 40 eV), 0.5 eV (40 eV $< h\nu <$ 80 eV) and 1 eV (80 eV $< h\nu <$ 210 eV). The photon energy resolution varied from ~5 meV at 10 eV to 100 meV at 210 eV. All the TOF spectra were recorded at room temperature. The fragment ion appearance energies, given in Table 2, were obtained from the ion yield spectra recorded as a function of photon energy. The quoted uncertainties have been based on the results obtained from the fitting procedure. However, if the rate constant for the production of a particular fragment ion is low at threshold, then the measured AE will be influenced by a kinetic shift. Under such circumstances the true AE may be substantially lower than the observed value.

Table 1
Isotope abundances taken from Kaye and Laby [15]

Element	Mass	Abundance (%)
Si	28	92.2
	29	4.7
	30	3.1
F	19	100
Cl	35	75.4
	37	24.6
Br	79	50.6
	81	49.4

3. Results and discussion

3.1. The overall spectra

The TOF spectra for SiF_4, plotted in Fig. 1, are similar to those reported in the two most recent

Table 2
Fragment ion appearance energies from previous and present work

Cation	Appearance energy (eV)					
	SiF_4		$SiCl_4$		$SiBr_4$	
	Previous work	This work[a]	Previous work	This work[a]	Previous work	This work[a]
SiX_3^+	15.5 [6], 16.1 [18], 16.20 [21], 16.2 [24]	16.15 ± 0.05	12.9 [19], 12.48 [20], 12.6 [22]	12.50 ± 0.05	11.31 [10]	11.05 ± 0.05
SiX_2^+	28 [6], 27.5 [18], 27.35 [21]	28.0 ± 0.8	18.1 [8], 18.4 [19], 17.64 [23]	18.1 ± 0.5	16.1 [10]	15.8 ± 0.7
SiX^+	26 [4], 29 [6], 28.75 [21]	28.9 ± 0.5	20.0 [9], 20.5 [19], 19.20 [23]	19.8 ± 0.5	17.1 [10]	17.1 ± 0.3
Si^+	37 [4], 36 [6]	35.5 ± 0.4	27 [19]	23.2 ± 0.4	23.4 [10]	20.7 ± 0.3
X^+	33 [4], 37 [6]	36.0 ± 0.8		21.0 ± 0.6	25.0 [10]	19.2 ± 0.4
X_2^+						27.0 ± 0.6
SiX_3^{2+}	40 [4], 50 [6]	41.0 ± 0.5	33.8 [19]	31.9 ± 0.5		31.5 ± 0.5
SiX_2^{2+}	42 [4], 45 [6]	42 ± 2	37.3 [19]	42 ± 2		42 ± 5
SiX^{2+}	51 [4], 54 [6]	51 ± 1	42 [19]	42 ± 1		70 ± 5
Si^{2+}	55 [4], 66 [6]	57 ± 2		59 ± 2		60 ± 2
X^{2+}	114.5 [7]	~105 ± 10		~190 ± 20		72 ± 5

[a] The quoted uncertainties have been based on the results obtained from the fitting procedure applied to the TOF spectra. However, if the rate constant for the production of a particular fragment ion is low at threshold, then the measured AE will be influenced by a kinetic shift. Under such circumstances the true AE may be substantially lower than the observed value.

studies [5,7], but the higher resolution attainable with the present apparatus allows the peaks due to the different Si isotopes to be resolved. To the best of our knowledge, a photoionisation mass spectrum of $SiCl_4$, recorded with monochromatic radiation, has not been published previously. The NIST database provides a mass spectrum, in the form of a histogram, obtained using electron impact at an energy of 70 eV [16]. However, this spectrum appears to show peaks due only to singly charged ions, even though the present work indicates that the energy used in the electron impact experiment exceeds the AEs for several of the doubly charged fragment ions. Very little information seems to be available regarding the mass spectrum of $SiBr_4$, and we are not aware of a published spectrum generated by either monochromatic radiation or energy selected electrons.

At low photon energies, where dissociation leads to fragments carrying away relatively small kinetic energies, peaks associated with different isotopic contributions to a specific fragment ion are easily resolved in the TOF spectrum. This is particularly evident in the spectra for $SiCl_4$ and $SiBr_4$, where the halogen atoms have two isotopes of significant abundance. However, at higher photon energies where the fragments may possess substantial kinetic energy, the resulting broadening in the TOF peaks leads to an overlap between the peaks associated with different isotopic species.

The spectra plotted in Figs. 1–3 show, as expected, that the degree of fragmentation increases as the photon energy increases. In addition, they reveal that the relative contributions from most of the atomic species (Si^+, Si^{2+} and X^+) become more significant for the heavier halogen atoms. This trend is not followed for X^{2+}, where the doubly charged halogen atomic ion is observed quite clearly in SiF_4 and $SiBr_4$, but only weakly in $SiCl_4$. For $SiBr_4$, the Br_2^+ fragment gives rise to a broad feature in the TOF spectrum, presumably due to the halogen molecular ion being formed with substantial kinetic energy. Santos et al. [5] observed a peak due to F_2^+ in their TOF mass spectrum of SiF_4. This molecular fragment was also detected, although with low intensity, in an early electron impact study [17]. However, the corresponding feature is not discernible in the more recent mass spectrum displayed in the NIST database [16]. The

present TOF spectra do not exhibit a peak which can be attributed to the F_2^+ fragment. Similarly, the TOF spectra for $SiCl_4$ do not contain a feature associated with the Cl_2^+ fragment.

For each of the three molecules, the TOF spectra recorded at high photon energies illustrate the propensity, observed previously for halogenated species [18], for the abundance of singly charged ions with an odd number of halogen atoms to be greater than the abundance of those with an even number. The relative intensities of the doubly charged fragment ions do not appear to follow a set pattern. It is evident that the ratio of the total intensity of doubly charged fragments to the total intensity of singly charged fragments decreases as the size of the halogen atom increases.

A summary of the present results is given in Table 2, together with the AEs from previous investigations. In our thermochemical estimations, the recommended heats of formation tabulated in the NIST Chemistry Database [16] have been used unless stated otherwise. However, due to the large disparity in the heats of formation for the silicon halides reported in the literature, the values employed in the present study have been listed in Table 3.

The following analysis is based primarily on a comparison between the experimentally measured AEs and the minimum energy requirement estimated from known thermochemical data. As this thermochemical estimation takes no account of the barriers in the reaction, the thresholds so obtained will always have a value lower than, or equal to, the AE. It is not unusual for such barriers to have energies as high as 1–2 eV. We can only estimate which fragmentation process produces the ion in question when that ion first appears. The number of accessible fragmentation channels increases as the molecular ion internal energy

Table 3
The heats of formation used in the present work

Species	Cation	Dication	Neutral	Anion
SiF_4	−129.7 ± 5.9 [31,33]		−1614.94 ± 0.8	
SiF_3	−120.1 ± 5.9 [31,33]		−1085.33 ± 16.7[d]	−1230 ± 46
SiF_2	410.0 ± 5.0 [31,33]	2284.5 [34]	−587.85 ± 12.6[d]	
SiF	641.4 ± 4.6 [31]	2715.4 [34]	−20.08 ± 12.6[d]	−103 ± 11
F_2	1514.5 ± 10 [35][a]		0	−291.0 ± 6.7
F	1760.5 ± 10 [35][a]		79.38 ± 0.3[d]	−248.6 ± 1.1 [28][e]
$SiCl_4$	526.7 ± 10 [35][a]		−662.75 ± 1.3[d]	
$SiCl_3$	426.8 ± 12.6 [29,30]		−390.37 ± 16.7[d]	−510.0 ± 9.2 [26]
$SiCl_2$	890 ± 10 [35][a]		−168.62 ± 3.3[d]	−228 ± 21
SiCl	905.5 ± 6.7 [32][b]		198.32 ± 6.7[d]	
Cl_2	1107.6 ± 10 [35][a]		0	−231.0 ± 19
Cl	1372.5 ± 10 [35][a]		121.30 ± 0.008	−227.4 ± 0.84
$SiBr_4$	940.7 ± 10 [35][a]		−415.47 ± 8.4[d]	
$SiBr_3$	531.6 ± 77 [10][c]		−201.69 ± 63[d]	
$SiBr_2$	∼768 [10][c]		−52.30 ± 16.7[d]	
SiBr	939.9 ± 10 [35][a]		235.33 ± 46[d]	
Br_2	1045.0 ± 10 [35][a]		31.0 ± 0.11	−215.0 ± 9.6 [25][f]
Br	1251.5 ± 10 [35][a]		111.87 ± 0.12	−212.8 ± 0.84
Si	1246 ± 2.9 [27,31,33]		450 ± 8	316.0 ± 7.9

[a] Experimental uncertainties for the heat of formation of the cation have not been given in the NIST Standard Reference Database 19A [35]. Hence a value of 10 kJ mol^{-1} has been assigned.

[b] Calculated using the ionisation energy (7.3296 eV) of SiCl measured by Marijnissen and ter Meulen [32].

[c] Calculated using the ionisation energy (7.6 eV) of $SiBr_3$ and (∼8.5 eV) of $SiBr_2$ measured by Creasey et al. [10].

[d] The heats of formation have been taken from the NIST Chemistry Webbook [16]. However, the experimental uncertainties have been taken from the original papers.

[e] Calculated using the electron affinity (3.40 eV) of F measured by Blondel et al. [28].

[f] Calculated using the electron affinity (2.55 eV) of Br_2 measured by Baeda [25].

(or incident photon energy) increases. The reaction kinetics of the dissociation process are also important, and this effect will be apparent in cases where the most thermochemically favourable fragmentation is kinetically unfavourable. Under such circumstances the observed AE will be higher than expected.

The singly and doubly charged fragment ions, observed in the photon energy range 10–210 eV, are listed in Tables 4 and 5, respectively, together with their AEs. Also included are the most pertinent fragmentation processes for the formation of a particular ion, together with the associated thermochemical thresholds. In addition, Table 5 contains estimated upper limits for the heats of formation, derived from the present experimental AEs, for ions where that information is presently unavailable. For the singly charged molecular ions with low AEs, production processes involving either photoionisation or ion-pair formation following photoexcitation are considered. We will discuss the singly charged ions first, in the order as listed in Table 4, and then the doubly charged ions as given in Table 5.

3.2. Fragment ion appearance energies and production mechanisms

3.2.1. Singly charged fragment ions

3.2.1.1. SiF_3^+, $SiCl_3^+$ and $SiBr_3^+$ (m/z ~85, ~136 and ~268). The SiX_3^+ fragments were observed strongly in the TOF spectra throughout the encompassed photon energy range, and the TOF peak profile consisted of several well resolved components associated with the various silicon and halogen atom isotopes. There are two fragmentation channels which may produce the SiX_3^+ ions. The first is photoionisation, followed by the elimination of a halogen atom from the excited SiX_4^+ cation (process (a)), whilst the second mechanism is dissociation into an ion-pair from excited neutral SiX_4 (process (b)).

$$SiX_4 + h\nu \rightarrow SiX_4^{+*} + e^-$$
$$SiX_4^{+*} \rightarrow SiX_3^+ + X \quad \text{(a)}$$

$$SiX_4 + h\nu \rightarrow SiX_4^* \rightarrow SiX_3^+ + X^- \quad \text{(b)}$$

The AE of SiF_3^+ was measured as 16.15 eV, which is in good agreement with the values obtained in three earlier studies [18,21,24], but significantly higher than that reported by Guo et al. [6]. The thermochemical threshold for process (a) lies above the AE. Furthermore, Ignacio and Schlegel [36] have calculated the AE for the SiF_3^+ fragment generated through process (a) and obtained a value of 16.25 eV. Yencha and Hopkirk [37] have studied the $SiF_3^+ + F^-$ ion-pair production process by detecting the F^- fragments, and observed an onset at 12.89 eV. The relative cross-section for F^- formation exhibited a maximum around 16 eV, which is close to the present AE for SiF_3^+. Thus, it appears that, at the observed onset of 16.15 eV, the SiF_3^+ fragments are formed through process (b) which has a thermochemical threshold of 12.92 eV. However, as the incident photon energy increases the ion-pair formation will not be able to compete effectively with the much stronger process of direct photoionisation.

In accord with earlier work [19,20,22], the AE of $SiCl_3^+$ was found to be 12.50 eV, and this value matches well with the thermochemical threshold of 12.55 ± 0.13 eV for direct photoionisation followed by the elimination of a chlorine atom. Ion-pair formation has an estimated thermochemical threshold, at 8.94 eV, lying significantly below the AE. Therefore, energy considerations indicate that, at threshold, the $SiCl_3^+$ fragment is formed through process (a).

The AE of 11.05 eV for the $SiBr_3^+$ fragment is slightly lower than that reported by Creasey et al. [10] but again is in good agreement with the thermochemical threshold of 10.98 ± 0.8 eV for direct photoionisation followed by the elimination of a bromine atom. The heats of formation for both the tribromosilyl and the dibromosilylene cations listed in the NIST Standard Reference Database 19A [35], ΔH_f ($SiBr_3^+$) = 1004.3 kJ mol^{-1} and ΔH_f ($SiBr_2^+$) = 1105.5 kJ mol^{-1}, appear to be far too high. Therefore, we have used values of 531.6 kJ mol^{-1} (ΔH_f ($SiBr_3^+$)) and ~768 kJ mol^{-1} (ΔH_f ($SiBr_2^+$)), calculated from the ionisation energies [10] of 7.6 eV ($SiBr_3$) and ~8.5 eV ($SiBr_2$), respectively, to estimate the thermochemical thresholds.

Table 4
Singly charged fragment ion appearance energies and the most pertinent thermochemical thresholds

Singly charged cation	Other fragments	SiF_4		$SiCl_4$		$SiBr_4$	
		Appearance energy (eV)[a]	Thermochemical threshold (eV)	Appearance energy (eV)[a]	Thermochemical threshold (eV)	Appearance energy (eV)[a]	Thermochemical threshold (eV)
SiX_3^+	$X (+e^-)$	16.15 ± 0.05	16.32 ± 0.03	12.50 ± 0.05	12.55 ± 0.13	11.05 ± 0.05	10.98 ± 0.8
	X^-		12.92 ± 0.03		8.94 ± 0.13		7.61 ± 0.8
SiX_2^+	$X_2 (+e^-)$	28.0 ± 0.8	20.99 ± 0.05	18.1 ± 0.5	16.09 ± 0.10	15.8 ± 0.7	~12.6
	$2X (+e^-)$		22.63 ± 0.05		18.61 ± 0.10		~14.6
	X_2^-		17.97 ± 0.09		13.70 ± 0.22		~10.0
	$X^- + X$		19.23 ± 0.05		14.99 ± 0.10		~11.2
SiX^+	$X_2 + X (+e^-)$	28.9 ± 0.5	24.21 ± 0.05	19.8 ± 0.5	17.51 ± 0.07	17.1 ± 0.3	15.53 ± 0.14
	$3X (+e^-)$		25.85 ± 0.05		20.03 ± 0.07		17.53 ± 0.14
	$X_2^- + X$		21.20 ± 0.08		15.12 ± 0.21		12.98 ± 0.17
	$X^- + X_2$		20.81 ± 0.05		13.90 ± 0.07		12.16 ± 0.14
	$X^- + 2X$		22.45 ± 0.05		16.41 ± 0.08		14.16 ± 0.14
Si^+	$2X_2 (+e^-)$	35.5 ± 0.4	29.65 ± 0.03	23.2 ± 0.4	19.78 ± 0.03	20.7 ± 0.3	17.86 ± 0.09
	$X_2 + 2X (+e^-)$		31.29 ± 0.03		22.30 ± 0.03		19.86 ± 0.09
	$4X (+e^-)$		32.94 ± 0.03		24.81 ± 0.03		21.86 ± 0.09
X_2^+	$SiX_2 (+e^-)$	Not observed		Not observed		27.0 ± 0.6	14.59 ± 0.22
	$SiX + X (+e^-)$						18.74 ± 0.50
	$Si + X_2 (+e^-)$						20.85 ± 0.16
	$Si + 2X (+e^-)$						22.85 ± 0.16
X^+	$SiX_3 (+e^-)$	36.0 ± 0.8	23.74 ± 0.20	21.0 ± 0.6	17.05 ± 0.20	19.2 ± 0.4	15.19 ± 0.67
	$SiX_2 + X (+e^-)$		29.72 ± 0.17		20.60 ± 0.11		17.89 ± 0.22
	$SiX + X_2 (+e^-)$		34.78 ± 0.17		23.15 ± 0.13		20.04 ± 0.50
	$SiX + 2X (+e^-)$		36.42 ± 0.17		25.66 ± 0.13		22.04 ± 0.50
	$Si + X_2 + X (+e^-)$		40.47 ± 0.13		27.02 ± 0.13		23.42 ± 0.16
	$Si + 3X (+e^-)$		42.12 ± 0.13		29.53 ± 0.13		25.42 ± 0.16

[a] The quoted uncertainties have been based on the results obtained from the fitting procedure applied to the TOF spectra. However, if the rate constant for the production of a particular fragment ion is low at threshold, then the measured AE will be influenced by a kinetic shift. Under such circumstances the true AE may be substantially lower than the observed value.

Table 5
Doubly charged fragment ion appearance energies and the most pertinent thermochemical thresholds

Dication	Other fragments	SiF_4			$SiCl_4$		$SiBr_4$	
		Appearance energy (eV)[a]	Thermochemical threshold (eV)	ΔH_f (dication) (kJ mol^{-1})	Appearance energy (eV)[a]	ΔH_f (dication) (kJ mol^{-1})	Appearance energy (eV)[a]	ΔH_f (dication) (kJ mol^{-1})
SiX_3^{2+}	X (+2e$^-$)	41.0 ± 0.5		≤2262	31.9 ± 0.5	≤2294	31.5 ± 0.5	≤2512
SiX_2^{2+}	X_2 (+2e$^-$)	42 ± 2	40.42		42 ± 2	≤3390	42 ± 5	≤3606
	2X (+2e$^-$)		42.06			≤3147		≤3413
SiX^{2+}	X_2 + X (+2e$^-$)	51 ± 1	45.70		42 ± 1	≤3268	70 ± 5	≤6196
	3X (+2e$^-$)		47.35			≤3026		≤6003
Si^{2+}		57 ± 2			59 ± 2		60 ± 2	
X^{2+}		~105 ± 10			~190 ± 20		72 ± 5	

[a] The quoted uncertainties have been based on the results obtained from the fitting procedure applied to the TOF specta. However, if the rate constant for the production of a particular fragment ion is low at threshold, then the measured AE will be influenced by a kinetic shift. Under such circumstances the true AE may be substantially lower than the observed value.

3.2.1.2. SiF_2^+, $SiCl_2^+$ and $SiBr_2^+$ (m/z ~66, ~100 and ~188). In all three molecules, the SiX_2^+ fragments gave rise to low intensity peaks in the TOF spectra and were much less abundant than the corresponding SiX_3^+ fragments. Four fragmentation channels may lead to the production of SiX_2^+. The first two processes (c) and (d) involve photoionisation followed by the elimination of a halogen molecule or two halogen atoms from excited SiX_4^+. In the second two processes (e) and (f), the SiX_2^+ fragments are formed through ion-pair production from excited SiX_4. However, ion-pair formation is expected to be weak in comparison with direct photoionisation.

$$SiX_4 + h\nu \rightarrow SiX_4^{+*} + e^-$$
$$SiX_4^{+*} \rightarrow SiX_2^+ + X_2 \quad \text{(c)}$$

$$SiX_4 + h\nu \rightarrow SiX_4^{+*} + e^-$$
$$SiX_4^{+*} \rightarrow SiX_2^+ + 2X \quad \text{(d)}$$

$$SiX_4 + h\nu \rightarrow SiX_4^* \rightarrow SiX_2^+ + X_2^- \quad \text{(e)}$$

$$SiX_4 + h\nu \rightarrow SiX_4^* \rightarrow SiX_2^+ + X^- + X \quad \text{(f)}$$

The AEs for SiF_2^+, $SiCl_2^+$ and $SiBr_2^+$ were determined to be 28.0, 18.1 and 15.8 eV, respectively. The present values are in accordance with previous work for both the SiF_2^+ [6,18,21] and $SiCl_2^+$ [9,19,23] species. Creasey et al. have reported an AE of 16.1 eV for $SiBr_2^+$ [10] which is slightly higher than the present result. All four processes (c)–(f) have thermochemical thresholds which lie below the AE, and therefore may produce the SiX_2^+ fragments. However, process (d) has the thermochemical threshold lying closest to the AE, and is also the most chemically intuitive.

3.2.1.3. SiF^+, $SiCl^+$ and $SiBr^+$ (m/z ~47, ~64 and ~108). Prominent peaks attributable to the SiX^+ fragments were evident in the TOF spectra of all three molecules and were significantly stronger than those due to the corresponding SiX_2^+ fragments. These observations are in accord with the propensity for detecting species with even or odd numbers of halogen atoms [18].

There are five fragmentation channels which may produce the SiX^+ ions. In two of these, photoionisation is followed by dissociation of excited SiX_4^+, whilst the other three involve ion-pair formation from excited SiX_4. Table 4 provides details of these processes and the corresponding thermochemical thresholds.

The AEs for SiF^+, $SiCl^+$ and $SiBr^+$ were 28.9, 19.8 and 17.1 eV, respectively, in reasonable agreement with most of the previous measurements [4,6,9,10,19,21,23]. In the formation of SiX^+, all of the fragmentation channels have thermochemical thresholds which are lower than the AE. In all cases, the channel whose threshold lies nearest to the AE is direct photoionisation followed by the elimination of three halogen atoms. In $SiBr^+$, the threshold for this channel lies slightly above the AE, but within the experimental uncertainty.

3.2.1.4. Si^+ (m/z ~28). The peak associated with the Si^+ fragment was clearly discernible in the TOF spectra of each molecule, and at high excitation energies was one of the strongest features. In the spectra recorded at 190 eV, it is noticeable that the relative contribution of the Si^+ peak to the total ion intensity increases significantly as the size of the halogen atom increases. The AEs of Si^+ from SiF_4, $SiCl_4$ and $SiBr_4$ were measured as 35.5, 23.2 and 20.7 eV, respectively. The present AE of Si^+ from SiF_4 agrees well with previous work [4,6]. This is not the case with the two other molecules, where the present AEs are several eV less than earlier values [10,19].

The Si^+ species can be formed by the three different processes (g)–(i). In the production of Si^+ from SiF_4, all three fragmentation channels have a thermochemical threshold which is less than the experimental AE. For $SiCl_4$ and $SiBr_4$, the threshold for process (g) lies above the appropriate AE, and therefore this channel cannot play a role in the formation of the Si^+ fragment just above threshold.

$$SiX_4 + h\nu \rightarrow SiX_4^{+*} + e^-$$
$$SiX_4^{+*} \rightarrow Si^+ + 4X \quad \text{(g)}$$

Processes (h) and (i), where the Si^+ fragments result from the dissociation of excited SiX_4^+, involve rearrangement reactions prior to the elimination of halogen species.

$$SiX_4 + h\nu \rightarrow SiX_4^{+*} + e^-$$
$$SiX_4^{+*} \rightarrow Si^+ + 2X_2 \quad \text{(h)}$$
$$SiX_4 + h\nu \rightarrow SiX_4^{+*} + e^-$$
$$SiX_4^{+*} \rightarrow Si^+ + X_2 + 2X \quad \text{(i)}$$

This indicates that in the formation of Si^+ from either $SiCl_4$ or $SiBr_4$, a rearrangement to form X_2 takes place if the precursor is the excited SiX_4^+ ion.

3.2.1.5. Br_2^+ (m/z ~160). The generation of the X_2^+ fragment requires a rearrangement to form a halogen–halogen bond prior to the breaking of the Si–X_2 bond. The X_2^+ species was observed only in the fragmentation of the $SiBr_4$ molecule, and had an AE of 27.0 eV. As far as we are aware, there has been no previous measurement of this AE. There are several fragmentation processes that result in the production of Br_2^+ and all have a thermochemical threshold which is at least 4 eV lower than the AE (Table 4).

3.2.1.6. F^+, Cl^+ and Br^+ (m/z 19, ~35.5 and ~80). A prominent peak due to the atomic halogen ion was observed in the TOF spectrum of each molecule. For a particular molecule, the relative contribution of the halogen atom peak in the TOF spectrum mirrored that associated with the Si^+ fragment, and in the spectrum of $SiBr_4$ recorded at 190 eV, the Br^+ peak is the most intense feature. The spectra shown in Figs. 1–3 illustrate that the TOF peak profile associated with the X^+ fragment changes shape as a function of photon energy. This issue will be discussed in greater detail in Section 3.3.

The AEs of F^+, Cl^+ and Br^+ from SiF_4, $SiCl_4$ and $SiBr_4$, respectively, were determined as 36.0, 21.0 and 19.2 eV. The present AE of F^+ is in good agreement with earlier values [4,6], but the AE of Br^+ is significantly lower than the value of 25.0 eV reported by Creasey et al. [10]. There are six fragmentation channels which may produce the X^+ fragments from SiX_4, and these are given in Table 4 together with the thermochemical thresholds where the relevant heats of formation of the ions and neutrals are available. Although some of the thermochemical thresholds lie above the AEs, there remain, even at the observed onset, three processes which may lead to the formation of the F^+ fragments, and two processes which may result in the Cl^+ or Br^+ species. For these latter two atomic ions, the production mechanism whose thermochemical threshold lies closest to the AE involves photoionisation followed by fragmentation into an X^+ ion and the neutrals SiX_2 and X.

3.2.2. Doubly charged fragment ions

There have been very few previous measurements of the AEs of doubly charged fragments from SiX_4. For SiF_4, the present results are in reasonable agreement with those reported by Imamura et al. [4], but tend to lie several eV lower than those determined in the electron impact studies of Guo et al. [6,7]. Vought has measured the AEs of $SiCl^{2+}$, $SiCl_2^{2+}$ and $SiCl_3^{2+}$ [19], with results similar to the present values. The TOF spectra recorded at 190 eV show that the ratio of the intensities in the peaks associated with the SiX^{2+}, SiX_2^{2+} and SiX_3^{2+} fragments is similar to the ratio of the intensities in the peaks associated with the corresponding singly charged ions, for X = Cl or Br. However, this pattern is not followed for SiF_4, where a prominent peak due to the SiF_2^{2+} fragment is observed.

As far as we are aware, heats of formation for SiX_n^{2+} ions have not been determined experimentally, although Hrusak et al. [34] have calculated ΔH_f (SiF^{2+}) and ΔH_f (SiF_2^{2+}). This lack of thermochemical data limits our ability to propose fragmentation mechanisms for the experimentally observed fragments. Apart from SiF^{2+} and SiF_2^{2+}, where use has been made of the theoretical values, the present AEs have been employed to deduce upper limits for the heats of formation of the doubly charged ions (Table 5).

3.2.2.1. SiF_3^{2+}, $SiCl_3^{2+}$ and $SiBr_3^{2+}$ (m/z ~42.5, ~68 and ~134). The SiX_3^{2+} fragments may be

formed through process (j), which is double photoionisation followed by the elimination of a halogen atom from excited SiX_4^{2+}.

$$SiX_4 + h\nu \rightarrow SiX_4^{2+*} + 2e^-$$
$$SiX_4^{2+*} \rightarrow SiX_3^{2+} + X \quad \text{(j)}$$

The AEs for SiF_3^{2+}, $SiCl_3^{2+}$ and $SiBr_3^{2+}$ were 41.0, 31.9 and 31.5 eV, respectively. These result in heats of formation of $\leq$2262 kJ mol^{-1} for SiF_3^{2+}, $\leq$2294 kJ mol^{-1} for $SiCl_3^{2+}$, and $\leq$2512 kJ mol^{-1} for $SiBr_3^{2+}$.

3.2.2.2. SiF_2^{2+}, $SiCl_2^{2+}$ and $SiBr_2^{2+}$ (m/z ~33, ~50 and ~94). The spectra recorded at high photon energies show that the relative intensity of the SiX_2^{2+} fragment peaks depends upon the identity of the halogen atom. In SiF_4, the SiF_2^{2+} peak is the strongest of the features associated with the doubly charged molecular fragments, whilst for $SiBr_4$, the peak due to $SiBr_2^{2+}$ is barely discernible. Thus, for $SiBr_2^{2+}$ in particular, the experimental onset was difficult to determine. There are two fragmentation channels which may produce the SiX_2^{2+} fragments. Both involve double photoionisation, and this is followed by the elimination of either a halogen molecule or two halogen atoms. An AE of 42 eV was deduced for all three SiX_2^{2+} fragments. Thus, for SiF_2^{2+}, the thermochemical thresholds for the two channels (Table 5) lie below the AE when the experimental uncertainty is taken into account. Alternatively, the present AE of SiF_2^{2+} may be used to derive ΔH_f (SiF_2^{2+}) and this yields values in the range $\leq$2437–2935 kJ mol^{-1}, depending on the production mechanism. These experimental results may be compared with the calculated value of 2284.5 kJ mol^{-1} [34].

Hrusak et al. [34] have calculated the double ionisation energy of SiF_2 and obtained a value of 29.70 eV. The present AE of SiF_2^{2+} can be used to deduce this double ionisation energy, and gives a result of 31.4 eV assuming that the neutral fragment produced in the dissociation process is molecular fluorine. The doubly charged states of SiF_2 have been investigated in a photofragmentation study performed by Lee et al. [38], and an electronic state of SiF_2^{2+} was identified lying 31.0 $\pm$ 0.5 eV above the ground state of the neutral molecule. Therefore, the two experimental values for the double ionisation energy are in excellent agreement.

The heats of formation derived from the AEs for $SiCl_2^{2+}$ and $SiBr_2^{2+}$ lie between $\leq$3147 and 3390 kJ mol^{-1} for ΔH_f ($SiCl_2^{2+}$), and $\leq$3413 and 3606 kJ mol^{-1} for ΔH_f ($SiBr_2^{2+}$).

3.2.2.3. SiF^{2+}, $SiCl^{2+}$ and $SiBr^{2+}$ (m/z ~23.5, ~32 and ~54). Figs. 1–3 show that the relative intensity of the SiX^{2+} fragment decreases as the size of the halogen atom increases. Although the peak due to SiX^{2+} is prominent in the mass spectrum of SiF_4, it is weak in the spectrum of $SiBr_4$. Two fragmentation channels may lead to the formation of the SiX^{2+} fragments, and details are provided in Table 5.

As the AE of SiF^{2+} was found to be 51 eV, both production mechanisms have thermochemical thresholds which are lower than the AE. The mechanism whose estimated threshold occurs closest to the AE involves double ionisation followed by the elimination of three fluorine atoms. Alternatively, the AE of SiF^{2+} can be used to derive an upper limit for the heat of formation of SiF^{2+}. The values so obtained lie in the range $\leq$3068–3845 kJ mol^{-1}, and may be compared with the theoretical result of 2715.4 kJ mol^{-1} [34]. The disparity between the experimental and computed heats of formation suggests that the experimental AE is influenced by a significant kinetic shift.

The double ionisation energy of SiF has been calculated as 28.33 eV by Hrusak et al. [34]. By using the present AE of SiF^{2+}, and assuming that three fluorine atoms are generated in the fragmentation process, a value of 32.0 eV can be obtained for this double ionisation energy. The ionisation energies of SiF and SiF^+ have been measured as 7.31 [39] and 21.7 [40], respectively, leading to a double ionisation energy of 29.0 eV.

The AEs of $SiCl^{2+}$ and $SiBr^{2+}$ were measured as 42 and 70 eV, respectively, and the heats of formation derived from the experimental AEs lie between $\leq$3026 and 3268 kJ mol^{-1} for $SiCl_2^+$, and $\leq$6003 and 6196 kJ mol^{-1} for $SiBr^{2+}$. The high value derived for

ΔH_f ($SiBr^{2+}$) indicates that the observed AE is influenced by a substantial kinetic shift.

3.2.2.4. Si^{2+}, F^{2+}, Cl^{2+} and Br^{2+} (m/z 14, ~19, ~35 and ~80). At high excitation energies the doubly charged atomic ions were observed, and their AEs are given in Table 5.

3.3. Fragment ion kinetic energies

It is well known [41–45] that an analysis of ion TOF peak shapes provides information concerning the initial kinetic energy possessed by the ion. Such analyses have been carried out on fragment ion peak shapes recorded in photoelectron–photoion coincidence studies and have yielded the average kinetic energy released during fragmentation [42]. If the incident photon energy is sufficient to generate a doubly charged parent ion that subsequently dissociates to form two singly charged species, then the TOF peak widths associated with these energetic fragments can be large [46]. The Coulomb repulsion between the two charged species results, typically, in initial kinetic energies of several eV, and fragment ions with such energies produce flat topped TOF peaks with sharply rising and falling edges. The base width of the essentially rectangular peak can then be related to the maximum initial translational energy possessed by the fragment [46].

The method used to introduce the gas into the spectrometer source region also affects the measured peak width [42,47]. If the gas enters through a narrow bore tube, then the molecular velocity distribution along the direction of the spectrometer axis can be narrower than thermal. The present spectrometer incorporates such an arrangement and this results in a reduced translational temperature.

Santos et al. [5] have characterised the initial kinetic energy, U_0, possessed by an ion using [41]

$$U_0 = \left[\frac{qE\,\Delta t}{2}\right]^2 \frac{1}{2m} \quad (1)$$

where q is the ion charge state, E the electric field in the source region, Δt the peak width (FWHM), and m in the mass of the ion. This expression assumes that the TOF analyser incorporates spatial focusing, and that there is no spread in the flight time due to the analyser itself. Unfortunately, Santos et al. have not stated the photon energy at which the TOF spectrum, used to obtain their quoted fragment ion kinetic energies, was recorded. As can be seen in Figs. 1–3, most of the fragment ion peak widths depend upon the excitation energy. In addition, some of the fragment ions exhibit a complicated peak shape which alters markedly with photon energy (see Fig. 4). Under such circumstances the kinetic energies derived using Eq. (1) can be misleading. For comparison with the results given by Santos et al., we use our TOF spectrum of SiF_4 measured at a photon energy of 190 eV, and consider only those ions whose peak shape does not alter with energy. It should be noted that even for these ions, the peak width varies with excitation energy. The kinetic energies obtained from the present data, using Eq. (1), are listed in Table 6, and are smaller than those given by Santos et al. Although the reduced translational temperature of the gas beam may account for part of this difference, some of the discrepancies appear too large to be attributed solely to this effect.

Some examples of fragment ion peak profiles changing with photon energy are shown in Fig. 4. The features associated with the halogen atomic ions (F^+, Cl^+ and Br^+) suggest that these species are being

Table 6
Maximum initial kinetic energy possessed by the parent and fragment ions in the TOF mass spectrum of SiF_4 recorded at a photon energy of 190 eV

Ion	Maximum initial kinetic energy (eV)	
	This work	Santos et al. [5]
Si^{2+}	0.54	2.1
SiF^{2+}	0.11	1.2
Si^+	0.14	1.0
SiF_2^{2+}	0.04	0.34
SiF_3^{2+}	0.03	0.18
SiF^+	0.13	1.1
SiF_2^+	0.17	1.1
SiF_3^+	0.02	0.07
SiF_4^+	0.02	0.04

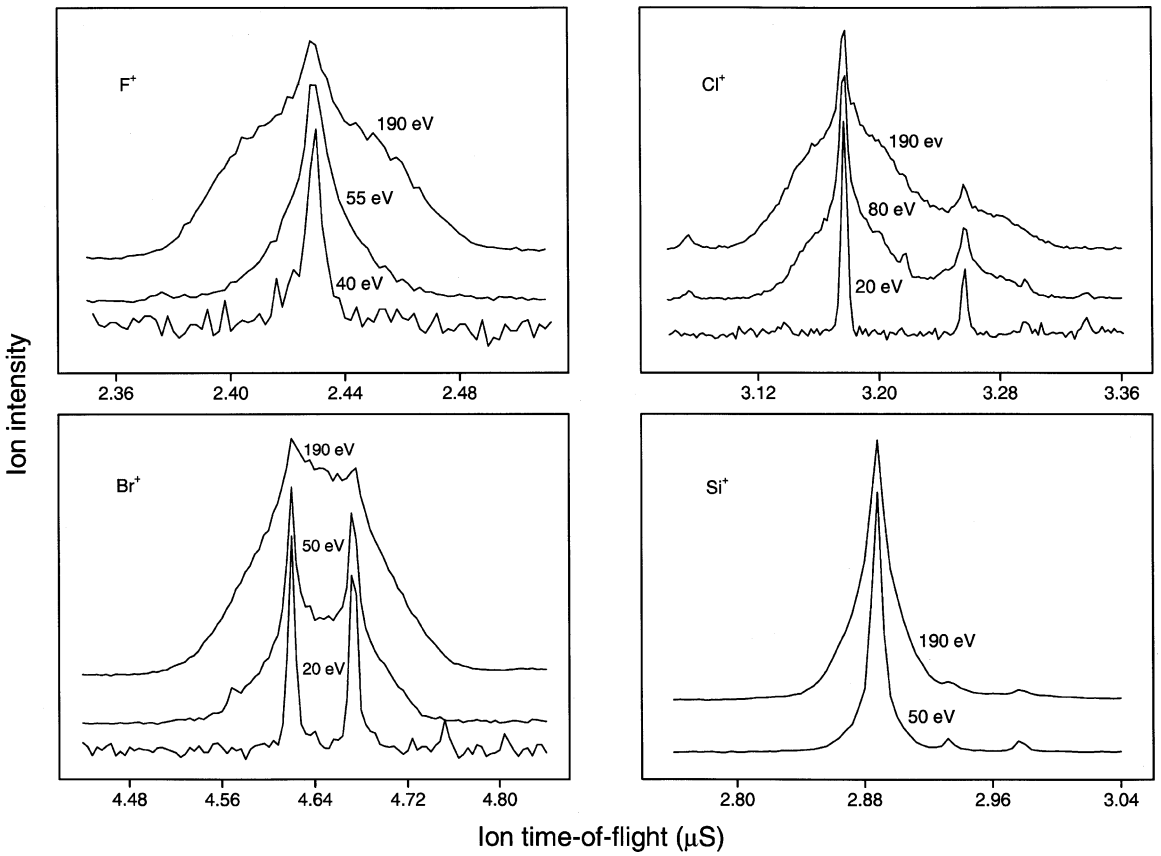

Fig. 4. TOF peaks, associated with the F^+, Cl^+, Br^+ and Si^+ fragments, illustrating the change in profile as a function of photon energy. The Si^+ fragments were produced from the fragmentation of $SiBr_4^+$. The photon energy at which each spectrum was recorded is marked in the figure.

formed through at least two processes, one of which releases little kinetic energy and leads to a narrow TOF peak, and a second in which substantial energy is released, resulting in a broad peak. An inspection of the peak shape reveals that the contribution due to the process releasing significant energy becomes more important as the photon energy increases. Fig. 4 shows that the TOF peak due to the F^+ fragment is narrow when the photon energy is only slightly greater than the AE of this species, but that the peak width has increased significantly for an excitation energy of 55 eV. The broadening continues as the photon energy increases but a noticeable enhancement occurs when the photon energy exceeds the ionisation threshold of the Si 2p subshell (∼112 eV). Once this threshold energy has been exceeded the peak shape remains approximately constant.

If it is assumed that the base width can be attributed to energetic ions travelling initially either directly towards or away from the detector, then an analysis of the TOF peak shape associated with the F^+ fragment shows that the initial maximum translational energy possessed by this species is about 9.5 eV. This energy has been deduced by computing ion flight times, as described previously [46], and not by using Eq. (1). The magnitude of the initial translational energy possessed by some of the F^+ fragments indicates that the energetic fragments are subject to a Coulomb repulsion. The peak due to the F^{2+} fragment also displays two components, one of which is narrow and

the other broad. The maximum translational energy associated with the broad component is about 7.6 eV. The thresholds for dissociative triple photoionisation of SiF_4 have been measured using photoion–photoion coincidence spectroscopy and occur at about 105 eV [3,4]. Therefore, it appears reasonable to associate the broad contribution to the F^{2+} TOF peak with a process involving Coulomb repulsion between this doubly charged species and an unidentified singly charged fragment.

It is more difficult to propose interpretations for the changes in the peak profiles observed in the TOF spectra of $SiCl_4$ or $SiBr_4$, due to the lack of complementary information. Furthermore, at high photon energies the interpretation, even for a particular fragment ion, is hampered by the overlap between the peaks due to the different halogen isotopes. Most of the TOF peaks become broader as the photon energy increases, and as an example, Fig. 4 shows the peak arising from the Si^+ fragment formed through the photoionisation of $SiBr_4$. An analysis of the Si^+ TOF peak shape, using the procedure already described for the F^+ fragment, shows that the maximum initial translational energy possessed by the Si^+ fragments is about 5.1 eV. At low photon energy the feature associated with $SiBr^+$ exhibits an easily resolvable doublet, corresponding with the two bromine isotopes, whereas at high photon energy Fig. 3 shows that the fragments possess substantially higher kinetic energies. The TOF peak profiles associated with the Cl^+ and Br^+ species exhibit a photon energy dependence similar to that displayed by the F^+ fragment. An analysis of the spectra shown in Fig. 4 reveals that, at a photon energy of 190 eV, the maximum initial translational energies possessed by the Cl^+ and Br^+ species are 11.0 and 12.1 eV, respectively.

4. Summary

Fragmentation processes occurring in SiF_4, $SiCl_4$ and $SiBr_4$, as a result of photon excitation in the energy range 10–210 eV, have been studied using TOF mass spectrometry. At high incident energies, the TOF spectrum of each molecule contains peaks associated with singly and doubly charged atomic and molecular fragments. Some of the fragments have been observed for the first time. AEs have been measured and, for the doubly charged species, used to derive upper limits for the heats of formation. For each fragment, a comparison has been made between the AE and the estimated thermochemical thresholds for the various fragmentation channels through which the fragment may be produced. In some cases this has allowed the mechanism responsible for generating the fragment at its threshold to be identified. The results indicate that some fragmentation mechanisms, for example, Br_2^+ or Si^+ from either $SiCl_4^+$ or $SiBr_4^+$, require a rearrangement of the ion structure to form a halide–halide bond prior to decomposition.

It appears that, at threshold, several of the larger, singly charged fragments may be produced through ion-pair formation rather than photoionisation. The interpretation of the present results relies heavily upon energetic considerations and is somewhat different to that proposed in a recent series of experiments [8–10]. In those studies it was suggested that the AEs of some of the smaller fragments correlated with the energies of excited electronic states rather than with thermochemical thresholds. Ion-pair formation was not invoked, and dynamical, rather than statistical, processes were considered to dominate the fragmentation.

The present TOF spectra show that the peaks due to several of the small fragments change shape as a function of excitation energy. Ion flight times have been computed and these have enabled initial kinetic energies to be determined.

Acknowledgements

We are grateful for financial support and a CASE studentship (L.C.) from the EPSRC, and for a Visiting Fellowship (L.G.S.) from the Royal Society.

References

[1] V.I. Nefedov, J. Struct. Chem. 11 (1970) 277.
[2] J.L. Dehmer, J. Chem. Phys. 56 (1972) 4496.

[3] P. Lablanquie, A.C.A. Souza, G.G.B. de Souza, P. Morin, I. Nenner, J. Chem. Phys. 90 (1989) 7078.
[4] T. Imamura, C.E. Brion, I. Koyano, T. Ibuki, T. Masuoka, J. Chem. Phys. 94 (1991) 4936.
[5] A.C.F. Santos, C.A. Lucas, G.G.B. de Souza, J. Electron Spectrosc. Relat. Phenom. 114–116 (2001) 115.
[6] X. Guo, G. Cooper, W.-F. Chan, G.R. Burton, C.E. Brion, Chem. Phys. 161 (1992) 453.
[7] X. Guo, G. Cooper, W.-F. Chan, G.R. Burton, C.E. Brion, Chem. Phys. 161 (1992) 471.
[8] D.M. Smith, R.P. Tuckett, K.R. Yoxall, K. Codling, P.A. Hatherly, Chem. Phys. Lett. 216 (1993) 493.
[9] D.M. Smith, R.P. Tuckett, K.R. Yoxall, K. Codling, P.A. Hatherly, J.F.M. Aarts, M. Stankiewicz, J. Chem. Phys. 101 (1994) 10559.
[10] J.C. Creasey, I.R. Lambert, R.P. Tuckett, K. Codling, L.J. Frasinski, P.A. Hatherly, M. Stankiewicz, J. Chem. Soc., Faraday Trans. 87 (1991) 3717.
[11] D.M.P. Holland, D.A. Shaw, I. Sumner, M.A. Hayes, R.A. Mackie, B. Wannberg, L.G. Shpinkova, E.E. Rennie, L. Cooper, C.A.F. Johnson, J.E. Parker, Nucl. Instrum. Meth. B179 (2001) 436.
[12] D.M.P. Holland, J.B. West, A.A. MacDowell, I.H. Munro, A.G. Beckett, Nucl. Instrum. Meth. B44 (1989) 233.
[13] P. Finetti, D.M.P. Holland, C.J. Latimer, C. Binns, F.M. Quinn, M.A. Bowler, A.F. Grant, C.S. Mythen, Nucl. Instrum. Meth. B184 (2001) 627.
[14] D.M.P. Holland, D.A. Shaw, I. Sumner, M.A. Hayes, R.A. Mackie, L.G. Shpinkova, L. Cooper, E.E. Rennie, J.E. Parker, C.A.F. Johnson, Int. J. Mass Spectrom., in press.
[15] G.W.C. Kaye, T.H. Laby, Tables of Physical and Chemical Constants, Longmans, London, 1966.
[16] NIST Chemistry Webbook (http://webbook.nist.gov/chemistry).
[17] H.J. Svec, G.R. Sparrow, J. Chem. Soc. A (1970) 1162.
[18] V.H. Dibeler, F.L. Mohler, J. Res. Natl. Bur. Stand. 40 (1948) 25.
[19] R.H. Vought, Phys. Rev. 71 (1947) 93.
[20] W.C. Steele, L.D. Nichols, F.G.A. Stone, J. Am. Chem. Soc. 84 (1962) 4441.
[21] J.P. McDonald, C.H. Williams, J.C. Thompson, J.L. Margrave, Adv. Chem. Ser. 72 (1968) 261.
[22] P. Potzinger, A. Ritter, J. Krause, Z. Naturforsch. 30a (1975) 347.
[23] H.R. Ihle, C.H. Wu, M. Miletic, K.F. Zmbov, Adv. Mass Spectrom. 7 (1978) 670.
[24] J.C. Creasey, I.R. Lambert, R.P. Tuckett, K. Codling, L.J. Frasinski, P.A. Hatherly, M. Stankiewicz, D.M.P. Holland, J. Chem. Phys. 93 (1990) 3295.
[25] A.P.M. Baeda, Physica 59 (1972) 541.
[26] R.E. Pabst, J.L. Margrave, J.L. Franklin, Int. J. Mass Spectrom. Ion Phys. 25 (1977) 361.
[27] M.E. Weber, P.B. Armentrout, J. Chem. Phys. 88 (1988) 6898.
[28] C. Blondel, P. Cacciani, C. Delsart, R. Trainham, Phys. Rev. A40 (1989) 3698.
[29] M.E. Weber, P.B. Armentrout, J. Phys. Chem. 93 (1989) 1596.
[30] E.R. Fisher, P.B. Armentrout, J. Phys. Chem. 95 (1991) 4765.
[31] E.R. Fisher, B.L. Kickel, P.B. Armentrout, J. Phys. Chem. 97 (1993) 10204.
[32] A. Marijnissen, J.J. ter Meulen, Chem. Phys. Lett. 263 (1996) 803.
[33] A. Ricca, C.W. Bauschlicher, J. Phys. Chem. A102 (1998) 876.
[34] J. Hrusak, Z. Herman, S. Iwata, Int. J. Mass Spectrom. 192 (1999) 165.
[35] NIST Standard Reference Database 19A.
[36] E.W. Ignacio, H.B. Schlegel, J. Phys. Chem. 94 (1990) 7439.
[37] A.J. Yencha, A. Hopkirk, J. Electron Spectrosc. Relat. Phenom. 79 (1996) 377.
[38] Y.-Y. Lee, S.R. Leone, P. Champkin, N. Kaltsoyannis, S.D. Price, J. Chem. Phys. 106 (1997) 7981.
[39] H. Bredohl, J. Breton, J. Dubois, J.M. Esteva, D. Macau-Hercot, F. Remy, J. Mol. Spectrosc. 195 (1999) 281.
[40] C. Heinemann, D. Schröder, H. Schwarz, J. Phys. Chem. 99 (1995) 16195.
[41] W.C. Wiley, I.H. McLaren, Rev. Sci. Instrum. 26 (1955) 1150.
[42] R. Stockbauer, Int. J. Mass Spectrom. Ion Phys. 25 (1977) 89.
[43] J.H.D. Eland, Mol. Phys. 61 (1987) 725.
[44] K. Codling, L.J. Frasinski, Contemp. Phys. 35 (1994) 243.
[45] T. Baer, W.L. Hase, Unimolecular Reaction Dynamics, Oxford University Press, Oxford, 1996.
[46] L. Cooper, L.G. Shpinkova, E.E. Rennie, D.M.P. Holland, D.A. Shaw, Int. J. Mass Spectrom. 207 (2001) 223.
[47] K.-M. Weitzel, J.A. Booze, T. Baer, Chem. Phys. 150 (1991) 263.